MUSCLE CO-CONTRACTION DURING ADAPTATION TO DYNAMIC PERTURBATIONS

By

Praveen Prabhakar Krishnan Ramaraj

A THESIS

Submitted to
Michigan State University
in partial fulfillment of the requirements
for the degree of

Kinesiology – Master of Science

2021

ABSTRACT

MUSCLE CO-CONTRACTION DURING ADAPTATION TO DYNAMIC PERTURBATIONS

By

Praveen Prabhakar Krishnan Ramaraj

In this study, participants performed center-out reaches to targets under the influence of a velocity dependent force field. They were assigned to one of two groups based on the type of perturbation: i) abrupt, and ii) gradual. The abrupt group was exposed to a force field of 20 $Nm^{-1}s$ whereas the gradual group was exposed to a force field that increased from 5 to 20 $Nm^{-1}s$ in increments of 5 $Nm^{-1}s$ every 52 trials. Muscle co-contraction was measured during the trials using two methods: i) Co-contraction Index, and ii) Global EMG. Our results suggest that the gradual group displayed a tendency to co-contract more during exposure to the force field. Post-exposure, the aftereffects remained for a short period of time with the gradual group tending to co-contract more. During the later part of post-exposure, no difference was seen between the two groups. In combination with the previously analysed kinematic data these results indicate that internal model acquisition and adaptation may be facilitated by muscle co-contraction and exposure to gradual dynamic perturbations as compared to abrupt dynamic perturbations.

ACKNOWLEDGMENTS

I would like to thank Dr. David Ferguson for his brilliant physiology classes and Dr. Rajiv Ranganathan for my first biomechanical analysis class. These classes were pivotal for me to form a full picture of my research. I would also like to thank them for being a part of my committee and giving me wonderful insights and feedback. I would like to thank my advisor, Dr. Florian Kagerer for guiding me with my thesis day and night and for always piquing my interest in neuroscience; I couldn't have asked for a better advisor. I want to thank David Ptashnik for directing me the right way, Henry Manoj D'Souza for the brainstorming sessions and Dr. Alex Brunfeldt for his guidance. I would like to thank my parents, K. Ramaraj and Jothi Visalakshi and my elder brother, Sibhi Siddarth; without their support and sacrifice, none of this would have been possible. Finally, I would like to thank Reshma Vijayan, for her unending support and optimism when it looked very hard; your motivation was crucial for this thesis. I would also like to thank my family and friends for their support!

TABLE OF CONTENTS

LIST OF TABLES

LIST OF FIGURES

CHAPTER 1

INTRODUCTION

In a novel dynamic perturbation environment, the central nervous system (CNS) uses muscle co-contraction to stabilize movement. Muscle co-contraction is the simultaneous contraction of the agonist and antagonist muscle spanning the same joint. It increases the stiffness of the limb and leads to increased accuracy and better pressure distribution over joint surfaces [Winter, 2009]. Excessive levels of muscle co-contraction can lead to poor motor performance, as seen in patients with neurological disorders, such as cerebral palsy, stroke, Parkinson's disease [Damiano et al., 2000; Rosa et al., 2014]. Even though it increases precision, muscle co-contraction can also be an inefficient mechanism in terms of energy requirement and can cause fatigue on prolonged use.

One of the tools used for studying muscle co-contraction is electromyography (EMG). It is a technique for recording the electrical activity of muscles, caused by the firing of the motor neuron during recruitment of a motor unit [Powers, 2020]. Examining and identifying signatures in muscle activity related to movement planning and execution, in turn, provides an insight into the muscular activation patterns produced by the nervous system. Due to the intricate nature of the sensorimotor system, much remains unknown about how it learns and controls voluntary movement. Multiple motor control theories have been proposed over time and the theory of internal models is the most prominent one among them. The idea of an internal model, first proposed by Francis and Wonham [1976] to be used in the engineering domain, was later adopted by neuroscientists. An internal model, simply put, is a theoretical representation of the sensory inputs and motor outputs of the sensorimotor system [Shadmehr et al., 2005]. Such a hypothesized representation mimics the neural machinery and makes it easier to understand how the nervous system functions and learns new tasks.

A common way to study motor control is to introduce perturbations during experiments while participants perform regular movements. A perturbation is any disturbance that causes the

system to behave differently and allows the researcher to study how the system responds and adapts to the perturbation. Visual and dynamic perturbations are commonly used for this purpose. The former is caused by altering the expected visual feedback from a movement whereas the latter involves application of a force field that deflects the normal movement trajectory of a reaching task. This allows studying the response of the motor system and its adaptation to the perturbations in order to counter it and move efficiently.

Visual and dynamic perturbations can be introduced either gradually or abruptly over the course of a movement task. In the case of dynamic perturbations, gradual perturbations involve introducing a weaker force field and increasing it in increments whereas abrupt perturbation starts out with a strong force field that remains constant throughout. For visual and dynamic perturbations, studies have shown that when perturbations are introduced gradually for one group and abruptly for another group, the gradual group displays a higher level of adaptation than the abrupt group [Kagerer et al., 1997; Klassen et al., 2005]. Similarly, muscle co-contraction is another mechanism that is shown to facilitate internal model acquisition [Heald et al., 2018]. It is, however, unknown whether these two mechanisms are related. The aim of our study was to determine the relationship between muscle co-contraction and adaptation to two different types of perturbation.

To gain an understanding of the acquisition and modification of internal models, EMG is used in conjunction with other techniques. These muscle activation recordings along with kinematics can provide an insight into the mechanisms used by the CNS for motor control. For the purpose of this thesis, data from a previously conducted study were used. In this study, participants were randomly assigned to either the gradual perturbation group or the abrupt perturbation group. EMG data were collected from three agonist-antagonist muscle pairs while they performed center-out reaches to three targets. We examined and re-analyzed the EMG signals and compared two methods to quantify muscle co-contraction. Muscle co-contraction levels were compared between the two groups along with kinematics to determine if gradual perturbation, which has been shown to lead to better adaptation, goes along with higher levels of muscle co-contraction.

CHAPTER 2

REVIEW OF THE LITERATURE

The human nervous system possesses the extraordinary capacity to maintain equilibrium in the body by adapting to external disturbances. Simple movements that we execute on a day-to-day basis require execution of multiple computationally complex steps by the nervous system. It is hypothesized that humans and some other animals build specific internal models in order to produce specific movements. Internal models are broadly classified into two types: i) Forward, and ii) Inverse [Wolpert et al., 1995, 1998; Kawato, 1999]. Forward internal models predict the next state of the system (such as position, velocity, etc.) based on the current state and the motor command whereas inverse internal models compute the feedforward motor command based on the desired trajectory.

Along with internal models and their characteristics, much interest lies in discovering the neural substrates involved in motor control. The cerebellum remains an area of significance in a large number of these studies as it is crucial for motor learning. Due to its highly uniform cytoarchitecture, it is believed that all the cerebellar areas facilitate a similar computational operation for extracerebellar regions. Studies indicate that internal models for eye movement are found in the cerebellum [Wolpert et al., 1998; Miall and Wolpert, 1996]. It is, however, unknown whether internal models for all movements are stored in the cerebellum [Ito, 1984].

In the context of the internal model theoretical concept, the CNS uses two control elements and combines them when performing reaching movements: i) feedback control, which uses visual and proprioceptive feedback after movement to estimate error, and ii) feedforward control, which makes predictions continuously about the next state of the system. These predictions are based on the current state of the system and the model of the movement that the CNS carries before the movement. Feedforward and feedback are crucial for motor learning and control. Feedback elements are inputs from the output of the movement itself, such as end-point error when the hands reach out to a target. This feedback can be used to form a better internal model of the

movement in its next iteration and minimize error.

As the internal model is built gradually with practice, the forward model becomes proficient in predicting the next state of the system [Thoroughman and Shadmehr, 1999]. In the study by Thoroughman and Shadmehr [1999], it was noticed that participants performed reaching movements by learning to predict the effect of the force field rather than responding to it through feedback. This forward mechanism is crucial to produce smooth coordinated movements because feedback control alone would be very slow, due to transmission delays in the nervous system.

2.1 Internal model – Gradual vs. Abrupt Perturbation

Dynamic perturbation such as a force field is introduced in experiments while performing reaching movements. A force field is a velocity-dependent resistive force against movement. Such an environment requires the CNS to adapt and predict the movement. As the task is being performed, the error made is being used to update the internal model. After exposure to the perturbations, their removal will show the extent of the adaptation the motor system has made to compensate for the dynamics [Shadmehr and Mussa-Ivaldi, 1994; Brashers-Krug et al., 1996].

While all participants display a level of adaptation, some types of perturbations facilitate a better adaptation from participants than others. In the study by Klassen et al. [2005], participants were divided into four groups – two groups were exposed to a visual perturbation (visuomotor rotation) and the other two groups were exposed to a dynamic perturbation (viscous force-field). For each type of perturbation, one group was exposed to gradually increasing dynamics that incremented to the final perturbation strength while the other group was abruptly exposed to the final perturbation strength. In both the visual and dynamic perturbation conditions, the gradual group displayed better adaptation and retained learning longer than the abrupt group.

Kagerer et al. [1997] reinforced this conclusion and showed that the adaptation is more pronounced when participants are exposed to gradually increasing perturbations as compared to abrupt perturbations. Two groups of participants made horizontal movements using a pen on a tablet to four different target locations. The visual feedback on the computer screen was rotated

90° counterclockwise. One group was exposed to a gradual increase of the visual feedback rotation from 0° to 90° in steps of 10°, whereas the other group was exposed to an abrupt rotation of 90°. It was observed that the group with a gradual increase in rotation had a smaller root mean square error (RMSE), movement time (MT) and initial directional error (IDE), as compared to the group with the abrupt perturbation. These results suggest that increasing the perturbation gradually rather than abruptly leads to more efficient updating of the internal model and better adaptation [Kagerer et al., 1997; Klassen et al., 2005].

2.2 Muscle co-contraction and internal model acquisition

While performing these reaching movements under novel dynamics, the nervous system co-contracts the agonist and antagonist muscle across the same joint. Muscle co-contraction is a mechanism used by the nervous system to manipulate the mechanical properties of the limb and provide movement stability when the limbs are subjected to external dynamic perturbations [Gribble et al., 2003; Milner, 2002; Rosa, 2014; Milner and Franklin, 2005]. Even though control of co-contraction is believed to be independent of movement, findings reveal that levels of co-contraction vary with movement velocity and amplitude [Gribble and Ostry, 1998; Darainy and Ostry, 2008]. It also increases in magnitude with the strength of the force field. Muscle co-contraction remains an integral part of total muscle activation even following learning and in a null force field.

Gribble et al. [2003] investigated the conditions under which the nervous system uses co-contraction and the relationship between co-contraction and movement accuracy required for the task. Participants were asked to point to targets that varied in size and location. When target size decreased, co-contraction increased and simultaneously trajectory variability decreased, and endpoint accuracy improved. As expected, speed decreased as target size decreased owing to the increased accuracy demand [Fitts, 1992; Harris and Wolpert, 1998].

Muscle co-contraction also accelerates the rate of internal model acquisition during reaching movements in the presence of novel dynamics [Heald et al., 2018]. This happens even though co-contraction reduces errors, which is considered to be a crucial input for acquiring a better

internal model. In this study, the authors pretrained three groups of participants using a sequence of force pulses – a stiff group instructed to co-contract during a dynamic perturbation, a relaxed group instructed to relax their arm muscles during a dynamic perturbation and a control group. The results showed that participants who were trained to co-contract their muscles while reaching under dynamic perturbation displayed higher adaptation, both in the initial and final stages of exposure. This suggested that muscle co-contraction improves the rate of dynamic motor learning despite reducing kinematic errors. Over the course of the study, as participants continued to adapt to the novel motor task, co-contraction went down [Heald et al., 2018; Thoroughman and Shadmehr, 1999; Osu et al., 2002].

This brings into question the reason the CNS uses co-contraction, even though it is a metabolically expensive mechanism. One possible theory that the nervous system chooses a trajectory to minimize the variance of the final position can be the reason it compromises on energy constraints and uses co-contraction to achieve it [Harris and Wolpert, 1998]. It has also been observed that the CNS uses co-contraction early while learning a novel motor task when an internal model has not been formed [Osu et al., 2002]. As learning takes place and a better internal representation is formed, co-contraction decreases, and the forward model can predict the outcome of the next state better. It is hypothesized that post learning, the increased stiffness might facilitate recollecting the appropriate internal model stored in the long-term memory [Thoroughman and Shadmehr, 1999].

2.3 Muscle co-contraction and gradual vs. abrupt perturbations

Studies have concluded that internal model acquisition is faster when participants are exposed to gradual perturbations compared to abrupt perturbations. On the other hand, previous studies have established that muscle co-contraction accelerates the rate of internal model acquisition [Heald et al., 2018; Gribble et al., 2003]. Not much is known whether these two mechanisms are related. Our study aims to check if there is a relationship between these two mechanisms. Participants were asked to perform reaching movements under the influence of gradual dynamic

perturbations and abrupt dynamic perturbations, using a Kinarm robotic manipulandum. During this task, kinematics data were derived from the robot, and EMG data were collected to make conclusions regarding adaptation, muscle activation patterns and co-contraction. If muscle co-contraction does facilitate better adaptation in the gradual perturbation, we expect to see participants in the gradual perturbation group have higher co-contraction, along with better adaptation to the perturbation.

2.4 EMG signal processing

In order to study this mechanism, it was essential to study the EMG signals of participants in the gradual and abrupt groups along with the kinematics. The main aim of this study was to find the best methods for EMG signal analysis and muscle co-contraction quantification to test our hypothesis.

Patients with neurological impairments such as stroke, cerebral palsy, Parkinson's disease, spasticity, etc. are often characterized by abnormal co-contraction of agonist and antagonist muscles. Muscle co-contraction is studied frequently in these patients to understand its importance in gait and postural stability [Unnithan et al., 1996; Chow et al., 2012; Rosa et al., 2014]. Rosa et al. [2014] reviewed these studies to answer three main research questions, i) What are the main characteristics of gait assessment protocols? ii) What are the main steps in the acquisition and analysis of surface electromyography (sEMG) signals? and iii) What parameters, formulas and computational approaches have been used to quantify muscle co-contraction? Of particular interest are the various methods used for the acquisition and analysis of sEMG (termed EMG in this document) signals and using computational approaches and formulas to quantify muscle co-contraction.

There is no one universal method employed for EMG signal analysis and quantifying muscle co-contraction levels. International Society of Electrophysiology and Kinesiology (ISEK) established standards for reporting EMG data to bring uniformity to EMG acquisition and analysis across studies [Merletti, 2018]. The standard specifies filtering sEMG signals within the range of 10-350 Hz, full-wave rectifying the signal and obtaining the Linear Envelope (LE) by low pass

filtering at 5 or 6 Hz [De Luca et al., 2010].

EMG normalization is an important step that is crucial for making comparisons between participants in a study. Raw EMG signals cannot be compared as the amplitude of EMG signals is meaningless and highly variable even across the same individual on different days. The amplitude of the signal is dependent on the participant, and they need to be normalized for comparison between participants in a study. The most common methods used for normalization are: i) Isometric maximal voluntary contraction (MVC), ii) Isokinetic MVC, iii) Peak dynamic method, iv) Mean dynamic method. Isometric and isokinetic MVCs are EMG measurements of individual muscles collected separately under maximal effort in isometric and isokinetic conditions. The maximum value is taken from the MVC signals of the respective muscles. This is used to normalize the EMG signals, dividing the amplitude by the maximum value. Peak and mean dynamic methods do not require separate data collection. The mean and peak values of the ensemble average of the EMG signals are used to normalize in the peak and mean dynamic method, respectively. Since mean and peak dynamic methods are performed using measures derived from normal movement, they cannot reveal how active a muscle is [Burden and Bartlett, 1999; Burden et al., 2003]. Isometric and isokinetic MVC normalization methods can provide a better estimate of how active a muscle is as the denominator in the normalization process is the maximum value under maximal effort.

Burden and Bartlett [1999] and Burden et al. [2003] compared the normalized EMG signals from these four methods to determine the best method for normalization. Burden and Bartlett [1999] calculated the root mean square difference (RMSD) between the methods and concluded that either the isometric MVC method or the isokinetic MVC method should be used for normalization. Burden et al. [2003] compared the same four methods and determined the method with the lowest inter-individual variability as the best one. It was noted that while peak and mean dynamic methods can remove inter-individual variability, they also remove the true variation in the signal. Isokinetic MVC does not reduce inter-individual variability. Isometric MVC was concluded to be the better method as it provides a better representation of muscle activation and reduced inter-individual variability.

Heald et al. [2018] normalized the EMG trace similar to the mean dynamic method by computing the mean of the early period EMG for each muscle during the baseline phase. The early period was defined to be 200 ms before movement onset and 130 ms after movement onset for each trial. This value was used to divide the EMG and scale it for comparison without affecting its temporal profile. This method was used in our study as the resulting EMG value after normalization provided an idea of muscle co-contraction with reference to the baseline phase where there were no dynamic perturbations.

2.5 Quantification of Muscle co-contraction

There is a lack of consensus on methods to quantify muscle co-contraction; therefore, different parameters and methods are used to determine co-contraction. For example, temporal muscle co-contraction was calculated by estimating the time the co-contracting muscles were active [Unnithan et al., 1996]. This study used two thresholds, 5% and 10% of the maximum of the MVC EMG signals to ascertain the muscles were active. Chow et al. [2012] estimated the duration of muscle co-contraction by dividing the time of overlap between active agonist and antagonist muscles by the phase duration and expressed it as a percentage. When the signal exceeded 3 SDs of the resting average EMG, the muscle was considered active [Chow et al., 2012]. The amount of muscle co-contraction was also determined using straightforward methods such as calculating the mean value of the area of overlap between the agonist and antagonist muscles, the correlation between the waveforms of the opposite muscles and the area of overlap between the two muscles.

Thoroughman and Shadmehr [1999] devised a new method to measure co-contraction and coined the term ‘wasted contraction’. They subtracted the amplitude of the smaller activity from the amplitude of the larger activity between the agonist-antagonist muscle pair at every sample point, thereby excluding the common activity that is cancelled by the opposite muscle and retaining only the activity that is essential for force production. Osu et al. [2002] proposed an index of muscle co-contraction around the joint (IMCJ) calculated using joint torque and sEMG signals.

Different methods were used to develop a quantitative index for muscle co-contraction,

mostly referred to as co-contraction index (CI):

i) dividing twice the common area of the LE between the antagonist and agonist muscle by the sum of the area of the two muscles and converting it to a percentage [Hesse et al., 2000; Winter, 2009; Kellis et al., 2003],

$$\%\ Co-contraction = 2\times\frac{Common\ area\ of\ the\ LE\ between\ the\ two\ opposite\ muscles}{Sum\ of\ area\ of\ the\ two\ opposing\ muscles}\times 100\% \quad (1)$$

ii) dividing the common area of the LE between the two opposite muscles by the number of data points [Unnithan et al., 1996; Kellis et al., 2003],

$$CI = \frac{Common\ area\ of\ the\ LE\ between\ the\ two\ opposite\ muscles}{Number\ of\ data\ points} \quad (2)$$

iii) dividing the common area of the LE between the two opposite muscles by the duration of the overlap [Chow et al., 2012],

$$CI = \frac{Common\ area\ of\ the\ LE\ between\ the\ two\ opposite\ muscles}{Duration\ of\ the\ overlap} \quad (3)$$

This index can in turn be used to estimate the magnitude of muscle co-contraction. Kellis et al. [2003] calculated the CI using four different methods. The first method was the one proposed by Hesse et al. [2000] and Winter [2009] [Equation 1], the second method was the one proposed by Unnithan et al. [1996] [Equation 2] and the third method was proposed by Chow et. al [2012] [Equation 3]. The fourth method involved calculating the CI at any point in time [Bowsher et al., 1993] using the following equations:

$$X_t = 1 - EMG_{AG} + EMG_{AT} \quad (4)$$

$$CI = [0.5 - (X_t + EMG_{ANT})X_t] \times 100 \tag{5}$$

where EMG_{AG} and EMG_{AT} are the EMG values of normalized linear envelopes of the agonist and antagonist muscles respectively at that point of time. EMG_{ANT} is the magnitude of the lowest EMG value of the two muscles at any instant in time. In the fifth method, the co-contraction index is calculated using the following equation:

$$CI = \frac{\int_{t1}^{t3} EMG_{BF}(t)\, dt}{\int_{t1}^{t3} [EMG_{RF} + EMG_{BF}](t)\, dt} \tag{6}$$

where EMG_{BF} and EMG_{RF} are the EMG values of normalized LEs of the biceps femoris and rectus femoris. Since the study by Kellis et al. [2003] examined the co-activation of the biceps femoris and rectus femoris while drop jumping, the equation is constructed for that purpose. The intervals $t1$ and $t3$ denote the entire period of activity of both the muscles.

The fifth method is based on the assumption that the biceps femoris acts as the stabilizer and the rectus femoris provides the main force for knee movement. It does not consider which muscle is the agonist and which muscle is the antagonist. Instead, it provides a measure of the contribution of the biceps femoris to total activation. With method 4, 100% co-contraction is achieved only when both the muscles are working at 100% MVC value. Due to these shortcomings, the first method was considered by Kellis et al. [2003] a more solid method with rationale behind it.

Heald et al. [2018] calculated a measure for co-contraction by deriving a global measure of muscle activity. Filtered, full-wave rectified signals were divided into early and late period EMG. These signals were normalized using the mean of baseline trials and averaged across time points. Global EMG measure was computed by calculating the difference between summed EMG across the muscles and summed baseline EMG across muscles for each trial. Negative values of global EMG indicate reduced co-contraction relative to the baseline phase of the experiment and positive values of global EMG indicate increased co-contraction relative to the baseline phase.

CHAPTER 3

HYPOTHESIS

Studies have suggested that internal model acquisition is faster when participants are exposed to gradual dynamic perturbation as compared to abrupt dynamic perturbations [Klassen et al., 2005]. While reaching under these novel dynamics, participants co-contract arm and shoulder muscles to increase stiffness and provide joint stability. If muscle co-contraction fastens internal model acquisition and adaptation to the task, then we hypothesize that participants in the gradual perturbation group will display better adaptation to the task and higher level of muscle co-contraction than participants in the abrupt perturbation group. This will establish muscle co-contraction as one of the main contributors to internal model acquisition. Alternatively, if the co-contraction levels are not higher in the gradual group, it might not be a contributing factor to adaptation.

CHAPTER 4

METHODS

Sixteen healthy college students (3 female; 13 right-handed; age 20.25 ± 2.13 yr., mean ± SD) from Michigan State University were recruited for this study. The experiment was approved by the Michigan State University Institutional Review Board. All participants reviewed and signed an informed consent statement before the experiment. Pre-collected data was used for this experiment [Ptashnik, 2019].

Participants made reaching movements using a robotic manipulandum (Kinarm by BKIN Technologies Ltd., Kingston, Ontario, Canada) [Figure 1] to three targets located 10 cm from the center and oriented at 45°, 90° and 135° from the center. Each block consisted of four trials, one each to targets at 45°, 90°, 135° and a channel trial to the 90° target, which was inserted between these regular reaches. In a channel trial, the force exerted against the channel wall was used to evaluate the level of adaptation. Target positions for the reaches and channel trials were selected at random for each block. Data from the robotic manipulandum were acquired at a sampling rate of 1000 Hz. The objective was to keep the reach durations between 800 ms and 1250 ms. Participants were provided colour feedback based on the timing after every trial – green if the reaching movement was within 800 ms and 1250 ms; blue if the movement was above 1250 ms; red if the movement was below 800 ms. Verbal feedback was also provided on increasing or decreasing speed for the blue or red colour feedback.

Participants were randomly assigned to one of two groups based on the type of dynamic perturbation: i) gradual, and ii) abrupt. All participants performed a total of 264 reaching trials, divided into three phases – i) Baseline, ii) Exposure and iii) Post-exposure. Both groups initially performed 28 unperturbed reaches as part of the baseline phase. This was followed by the exposure phase that consisted of 208 trials with dynamic force perturbations. The gradual group experienced perturbations of 5, 10, 15, 20 $\mathrm{Nm^{-1}s}$ in increments every 52 trials. The abrupt group, on the other hand, experienced perturbation of 20 $\mathrm{Nm^{-1}s}$ from the beginning and throughout the 208 trials.

Figure 1: Representative image of a KINARM apparatus by BKIN Technologies.

This exposure phase was followed by the post-exposure phase consisting of 28 unperturbed trials, in order to assess the level of adaptation attained by the participants.

EMG signals were recorded for all the trials to study the level of co-contraction and compare it with the kinematic data. The EMG signals were recorded using a BrainVision ExG 16 channel Brain Amp system (Brain Products, Gilching, Bavaria, Germany) with a sampling rate of 1000 Hz and containing six channels of data, one for each muscle of interest (see Table 1). The main purpose of this study was to re-assess the EMG data and measure muscle co-contraction levels from the EMG signals.

In the current study, EMG signals were analyzed based on ISEK standards. EMG signals were filtered using the *filtfilt* function in MATLAB R2019a. A 10^{th} order bandpass Butterworth filter was used between 10 Hz and 350 Hz. The signal was then full-wave rectified. In order to acquire a linear envelope of the signal, it was low pass filtered at 6 Hz using a 2^{nd} order Butterworth filter. The *filtfilt* function in Matlab was used for this as well. After this point, we used two different approaches to quantify muscle co-contraction – i) Global EMG method based on the work of Heald

et al. [2018] and ii) CI method based on the work of Hesse et al. [2000], Winter [2009] and Kellis et al. [2003].

Channel	Muscle
1	Biceps
2	Triceps
3	Posterior Deltoid
4	Anterior Deltoid
5	Trapezius
6	Pectoralis Major

Table 1: Channel layout used for EMG.

4.1 Co-contraction Index method

The procedure used to process the EMG signals (filter, full-wave rectification, and linear envelope) was followed to process the isometric MVC data as well. The maximum value from each muscle's isometric MVC signal was obtained. The rectified linear envelope of the EMG signal was then normalized by dividing it with this maximum value. The data for each muscle in a trial was divided into two separate epochs based on markers for the start of the trial (T1), movement onset (B1) and movement offset (U1). The first epoch was cut from movement onset (B1) to movement offset (U1). The second type involved extracting epochs 500 ms before movement onset (B1). This was done to analyze the movement planning phase prior to movement onset.

The epochs between movement onset and offset from the first method were used to calculate the co-contraction index (CI) for both the abrupt and gradual groups. For each epoch, only the values that were equal to or above 5% of the maximum isometric MVC value were obtained. This was done to ensure that only active muscle data was used for calculation of the CI. The lowest value between the agonist and antagonist muscle signal was calculated and stored at every time point. This provided an overlap curve between the agonist and antagonist when both the muscles were active. The CI was calculated using the following formula for each epoch:

$$CI = \frac{\int_{B1}^{U1} EMG_{OL}(t)\, dt}{(\int_{B1}^{U1} EMG_{AG}(t)\, dt + \int_{B1}^{U1} EMG_{AT}(t)\, dt)} \tag{7}$$

where B1 and U1 denote movement onset and offset and are also indicative of the start and end of each epoch. EMG_{AG}, EMG_{AT} and EMG_{OL} are EMG signals of the agonist muscle, antagonist muscle and overlap between the agonist and antagonist muscles, respectively. The CI was determined for each epoch and the mean of this was calculated for the different phases (baseline, exposure, and post-exposure) of every participant.

4.2 Global EMG method

The linear envelope of the EMG signals was divided into epochs over two periods: i) early, and ii) late. For each trial, the early period was taken from 200 ms before movement onset (B1 marker) to 130 ms after movement onset (B1). The late period, on the other hand, was from 130 ms to 400 ms after movement onset (B1). The early period was used as a measure of feedforward control as feedback components are usually seen around 130 ms after movement onset. The mean of the early period of the non-channel trials during the baseline phase was computed for each muscle separately. This value was used to divide the EMG trace of both the early and late period of each muscle for every trial to normalize them.

Baseline EMG signals were first averaged across time points and then across trials. The values obtained were summed across muscles to obtain a baseline value. EMG signals were simultaneously averaged across time points for each trial and then summed across muscles such that each trial had an independent value. Global EMG was calculated by taking the difference between this value and the baseline value. These steps were carried out individually for both early and late periods of the EMG signals. Global EMG denotes muscle activity and stiffness relative to the baseline phase where there were no dynamic perturbations. A positive value signifies higher activity than baseline EMG and a negative value signifies lower activity than baseline EMG.

4.3 EMG Analysis

Average of the global EMG and CI were calculated for every participant in both the groups across different phases of the experiment: i) baseline phase (last 20 trials – 15 non-channel trials and 5 channel trials), ii) exposure phase (last 20 trials – 15 non-channel trials and 5 channel trials), iii) early post-exposure phase (first 12 trials – 9 non-channel trials and 3 channel trials) and iv) late post-exposure phase (last 12 trials – 9 non-channel trials and 3 channel trials). The averages were calculated separately for channel and non-channel trials. These values were used for statistical analysis. The average of the trials for the baseline phase of global EMG were excluded for analysis as the measure itself was relative to the baseline. It was noticed that in some muscles and participants the MVC values were not representative of the maximal contraction possible. Hence the normalization process using isometric MVC and the resultant CI were not entirely reliable. Due to this reason, global EMG was used as the primary index for assessing co-contraction in this study.

To identify differences in muscle co-contraction (CI and Global EMG) between the abrupt and gradual groups, repeated measures ANOVAs, one-tailed t-tests and two-tailed t-tests were performed with significance set to $p < 0.05$. Data was rounded down to 3 decimal points and reported as mean ± standard deviation unless mentioned otherwise.

CHAPTER 5

RESULTS

Participants started by performing center-out reaches to three targets along with force channel trials in a null field during the baseline phase. This was followed by the exposure phase with the introduction of dynamic force perturbations –20 $Nm^{-1}s$ for the abrupt group and increments of 5, 10, 15, 20 $Nm^{-1}s$ every 52 trials for the gradual group. The perturbations were then removed to assess the level of adaptation during the post-exposure phase. Muscle co-contraction was calculated for all the trials and comparisons were made between the abrupt and gradual group through the different phases.

5.1 Co-contraction Index method

CI was calculated between the agonist-antagonist pairs – 1. biceps & triceps, 2. posterior & anterior deltoid, and 3. trapezius & pectoralis major, for every trial. Figures 2 and 3 show the CI levels of each block for channel and non-channel trials, respectively. During the analysis, it was noticed that the maximum isometric MVC value for some muscles were significantly lower than the amplitude values of the EMG signal. Isometric MVC normalized EMG signals are expressed as a fraction of the maximum value, and this enables comparison between participants. The normalized signals in our study were not relative to the maximum amplitude value of the participants and due to this, valid comparisons between participants are likely compromised. This problem was noticed regularly for the EMG signals of the trapezius and pectoralis major; therefore, this pair was not included in the statistical analysis.

5.1.1 Baseline EMG

During baseline, co-contraction index between the two groups was similar. The CI between the biceps and triceps (abrupt: n = 8, 0.765 ± 0.273; gradual: n = 8, 0.740 ± 0.271) of the non-channel trials during the baseline was very similar (two-tailed t-test: $t_{14} = 0.187$, P = 0.854).

Similarly, the CI of non-channel trials was very similar between the posterior and anterior deltoid (abrupt: n = 8, 0.820 ± 0.265; gradual: n = 8, 0.925 ± 0.910) during baseline (two-tailed t-test: t_{14} = -0.488, P = 0.633). This showed that co-contraction between the two groups was similar before the introduction of force perturbations.

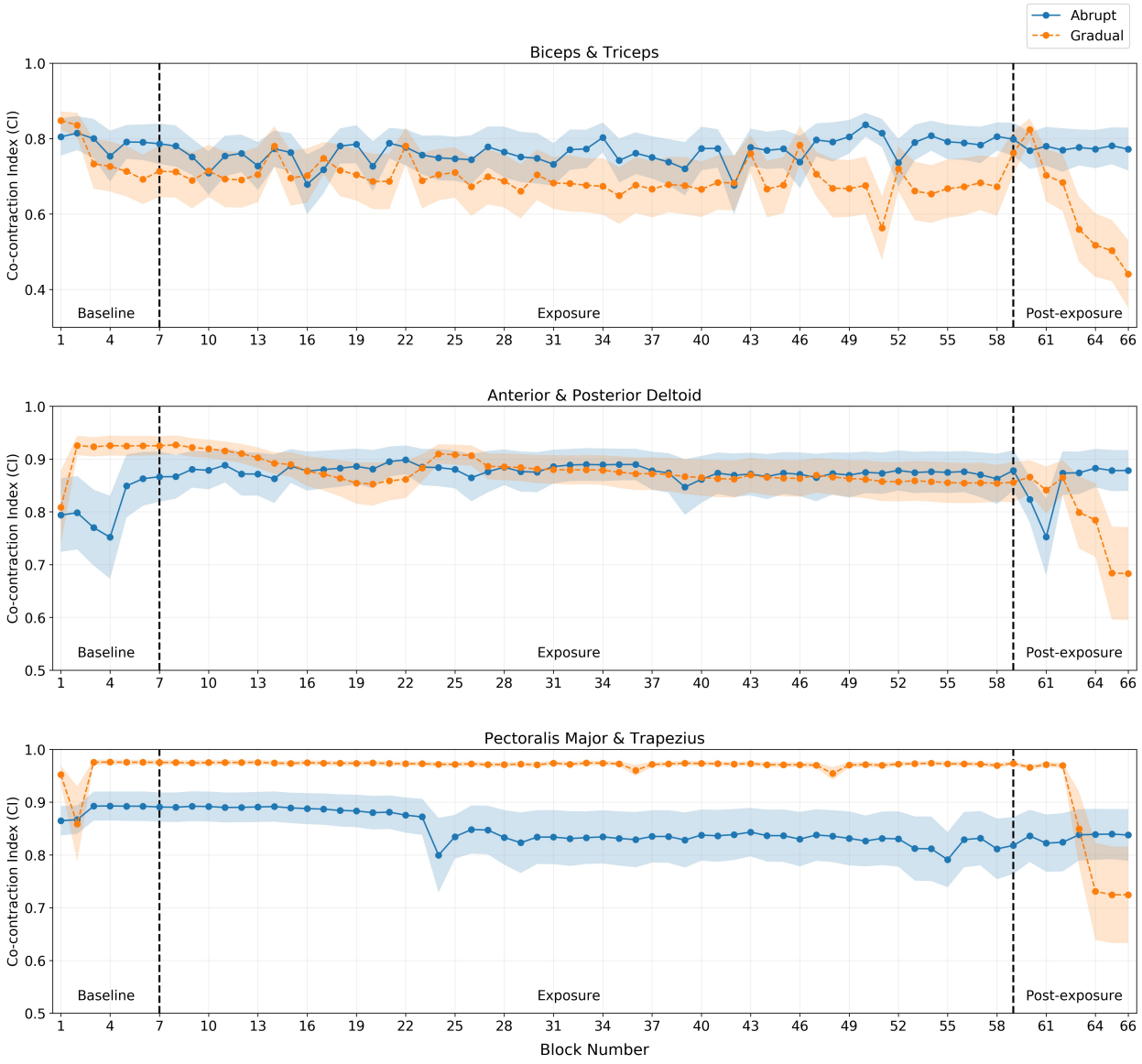

Figure 2: Co-contraction Index of channel trials for every block. Data shows mean ± standard error. The ceiling effect for the gradual group in the bottom panel was found to be due to incorrect MVC recordings; this muscle pair was therefore excluded from further analysis.

5.1.2 Exposure EMG

The mean of the last 15 non-channel trials and 5 channel trials of the exposure phase was calculated individually and used to compare CI between the two groups. CI between the biceps and triceps did not exhibit any major differences between the two groups for channel trials (abrupt: n = 8, 0.794 ± 0.212; gradual: n = 8, 0.691 ± 0.336; one-tailed t-test: $t_{14} = 0.727$, P = 0.240) and non-channel trials (abrupt: n = 8, 0.780 ± 0.242; gradual: n = 8, 0.683 ± 0.342; one-tailed t-test: $t_{14} = 0.656$, P = 0.261). No difference was noticed between the CI of the two groups for the anterior and posterior deltoid for both channel trials (abrupt: n = 8, 0.872 ± 0.202; gradual: n = 8, 0.855 ± 0.184; one-tailed t-test: $t_{14} = 0.181$, P = 0.430) and non-channel trials (abrupt: n = 8, 0.874 ± 0.198; gradual: n = 8, 0.858 ± 0.180; one-tailed t-test: $t_{14} = 0.178$, P = 0.431). Even though both the abrupt and gradual groups experienced 20 $Nm^{-1}s$ during the last 20 trials of exposure, the gradual group was expected to have a higher CI due to the incremental nature of the force field.

5.1.3 Post-Exposure EMG

During the course of early and late post-exposure, there was a tendency towards a main effect for time during the channel trials of the biceps and triceps ($F_{1,14} = 3.637$, P = 0.077). There was no main effect for group ($F_{1,14} = 1.612$, P = 0.225). There was a tendency for a group by time interaction in the channel trials of both the biceps and triceps (abrupt: n = 8, mean ± standard error = 0.774 ± 0.090; gradual: n = 8, mean ± standard error = 0.774 ± 0.090; $F_{1,14} = 3.789$, P = 0.072) and the anterior and posterior deltoid (abrupt: n = 8, mean ± standard error = 0.848 ± 0.081; gradual: n = 8, mean ± standard error = 0.787 ± 0.081; $F_{1,14} = 3.616$, P = 0.078). The channel trials of the anterior and posterior deltoid did not display any main effect for time ($F_{1,14} = 0.514$, P = 0.485) or group ($F_{1,14} = 0.284$, P = 0.602). Similarly, no group by time interaction was found for the non-channel trials of the biceps and triceps (abrupt: n = 8, mean ± standard error = 0.771 ± 0.090; gradual: n = 8, mean ± standard error = 0.612 ± 0.090; $F_{1,14} = 2.304$, P = 0.151) or the anterior and posterior deltoid (abrupt: n = 8, mean ± standard error = 0.875 ± 0.077; gradual: n = 8, mean ± standard error = 0.805 ± 0.077; $F_{1,14} = 2.564$, P = 0.132). Further, main effects for

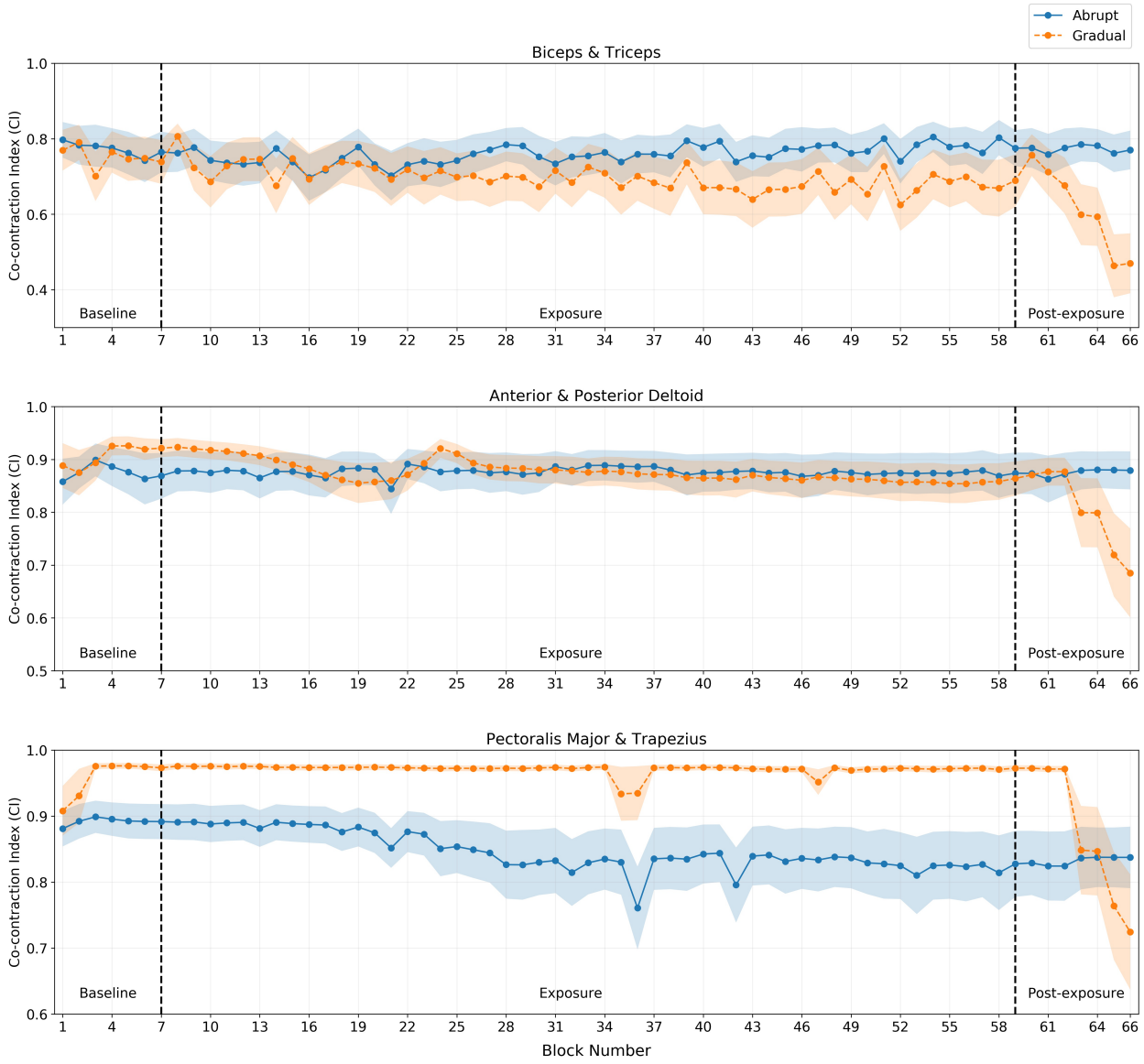

Figure 3: Co-contraction Index of non- channel trials for every block. Data shows mean ± standard error.

time ($F_{1,14}$ = 2.255, P = 0.155) and group ($F_{1,14}$ = 1.570, P = 0.231) for the non-channel trials of the biceps and triceps along with main effects for time ($F_{1,14}$ = 1.908, P = 0.189) and group ($F_{1,14}$ = 0.416, P = 0.529) for the non-channel trials of the anterior and posterior deltoid were absent.

5.2 Global EMG method

Global EMG was obtained from normalized EMG signals, as seen in Figure 4 and divided into early and late periods; both the periods were used separately for analysis.

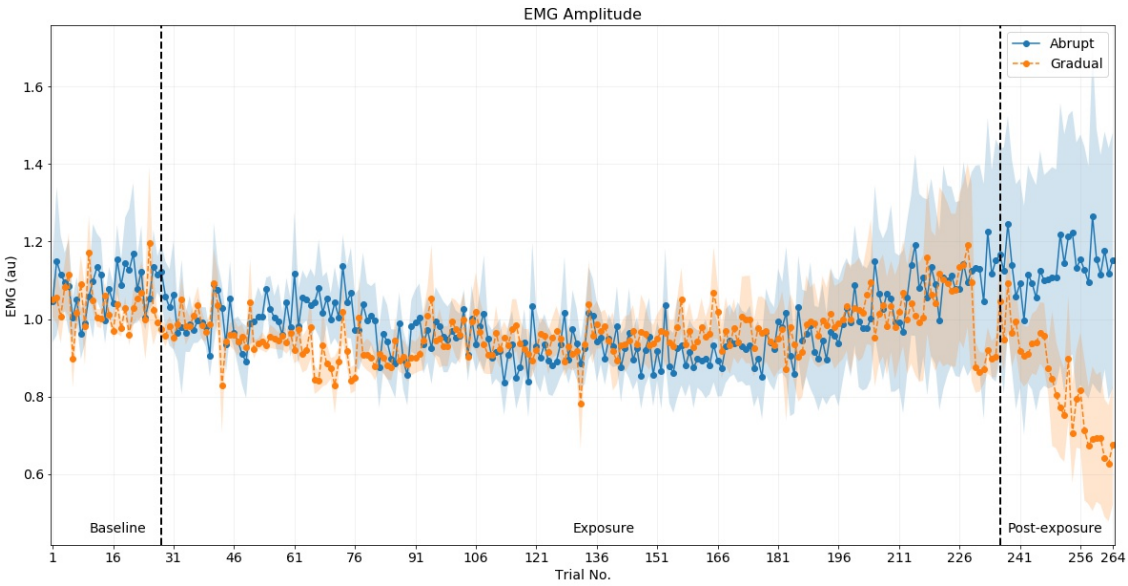

Figure 4: Normalized amplitude of EMG during the late EMG period. EMG is in arbitrary units (au). Data shows mean ± standard error.

The average global EMG values were calculated for every trial for each participant and then a few trials indicative of a phase were averaged. It was noticed that one of the participants from the abrupt group displayed values that differed significantly from other participants and were likely due to a recording artifact. Due to this, the data from that participant was concluded to be an outlier and removed for statistical analysis. Since global EMG is a measure of co-contraction relative to baseline, statistical analysis of baseline was not performed.

5.2.1 Exposure EMG

During the late part of the exposure phase (last 20 trials – 15 non-channel trials, 5 channel trials), both abrupt and gradual group experienced a force perturbation of 20 $Nm^{-1}s$. During the early EMG period of these trials, the gradual group displayed a tendency to co-contract more to counter the force field for channel (abrupt: n = 7, -1.220 ± 1.218; gradual: n= 8, 0.543 ± 3.210; t_{13} = -1.365, one-tailed t-test: P = 0.098; two-tailed t-test: P = 0.195) and non-channel (abrupt: n = 7, -1.223 ± 1.331; gradual: n = 8, 0.111 ± 2.156; t_{13} = -1.415, one-tailed t-test: P = 0.090; two-tailed t-test: P = 0.181) trials.

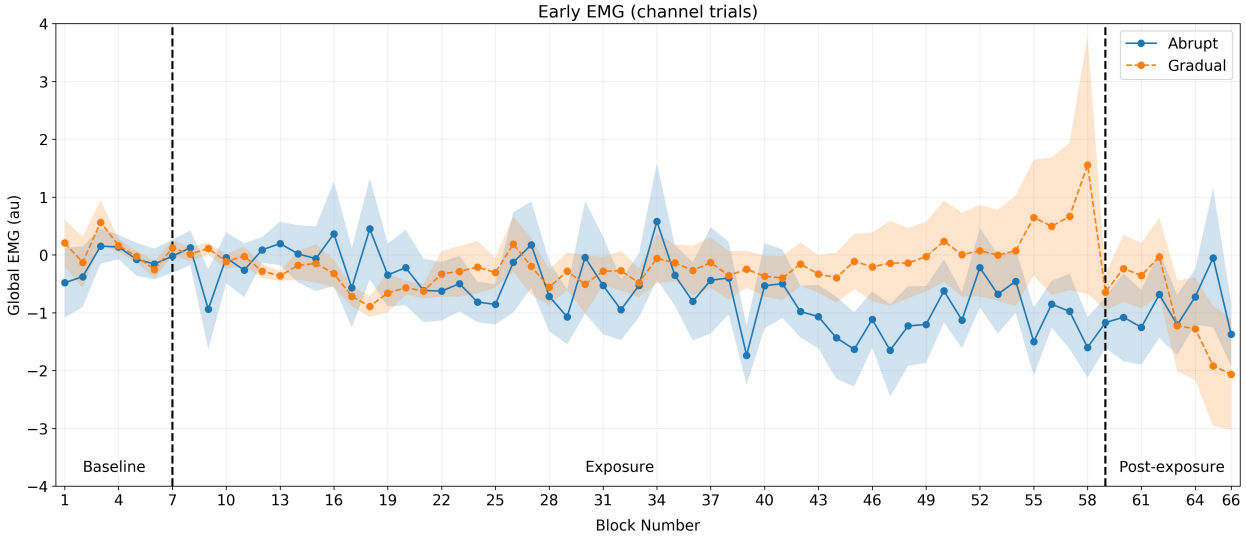

Figure 5: Global EMG of channel trials during the early EMG period. Global EMG is in arbitrary units (au). Data shows mean ± standard error.

This was significant during the late EMG period for the channel (abrupt: n = 7, -1.899 ± 1.801; gradual: n = 8, 0.354 ± 2.647; t_{13} = -1.896, one-tailed t-test: P = 0.040; two-tailed t-test: P = 0.080) trials, as seen in Figure 7. A similar tendency was noticed for the non-channel (abrupt: n = 7, -1.510 ± 1.767; gradual: n = 8, -0.062 ± 2.088; t_{13} = -1.438, one-tailed t-test: P = 0.087; two-tailed t-test: P = 0.174) trials during the late period. This supports our hypothesis that the gradual group co-contracted higher than the abrupt group, even under the same force field strength.

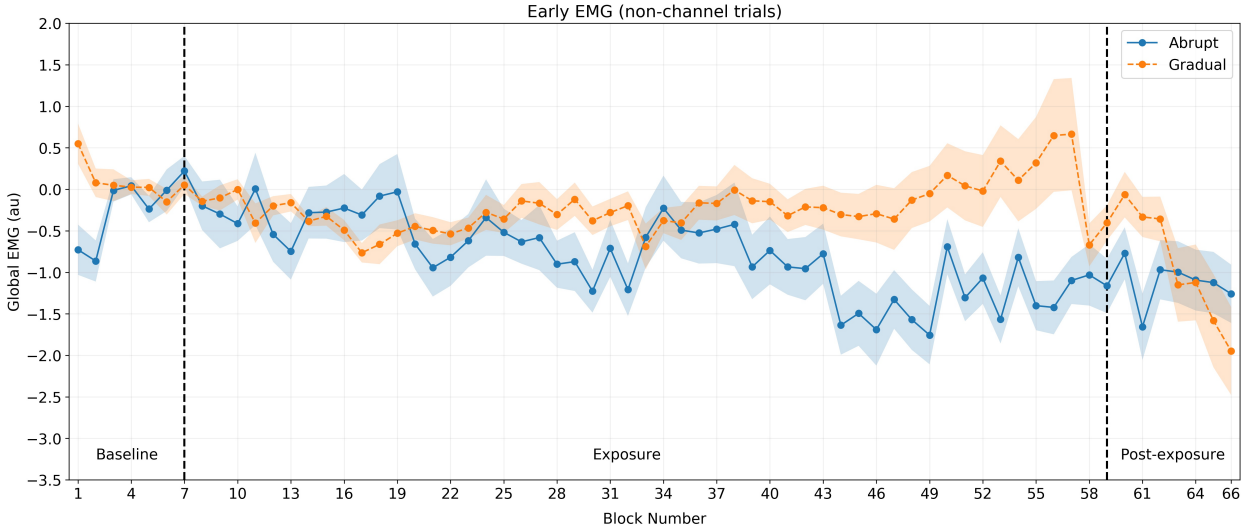

Figure 6: Global EMG of non-channel trials during the early EMG period. Global EMG is in arbitrary units (au). Data shows mean ± standard error.

5.2.2 Post-exposure EMG

During the early part of post-exposure (first 12 trials – 9 non-channel trials, 3 channel trials), when the force perturbation was removed, the same tendency for the gradual group to co-contract more than the abrupt group was present in both the channel trials (abrupt: n = 7, -1.790 ± 2.160; gradual: n = 8, -0.607 ± 1.041; t_{13} = -1.382, one-tailed t-test: P = 0.095; two-tailed t-test: P = 0.190) and non-channel trials (abrupt: n = 7, -1.488 ± 1.717; gradual: n = 8, -0.298 ± 1.225; t_{13} = -1.562, one-tailed t-test: P = 0.071; two-tailed t-test: P = 0.142) of the late EMG period, as seen in Figure 7 and 8. This did not hold for the channel (abrupt: n = 7, -1.006 ± 1.790; gradual: n = 8, -0.209 ± 1.439; t_{13} = -0.956, one-tailed t-test: P = 0.178; two-tailed t-test: P = 0.357) and non-channel (abrupt: n = 7, -1.132 ± 1.361; gradual: n = 8, -0.252 ± 1.268; t_{13} = -1.297, one-tailed t-test: P = 0.109; two-tailed t-test: P = 0.217) trials of the early period of EMG.

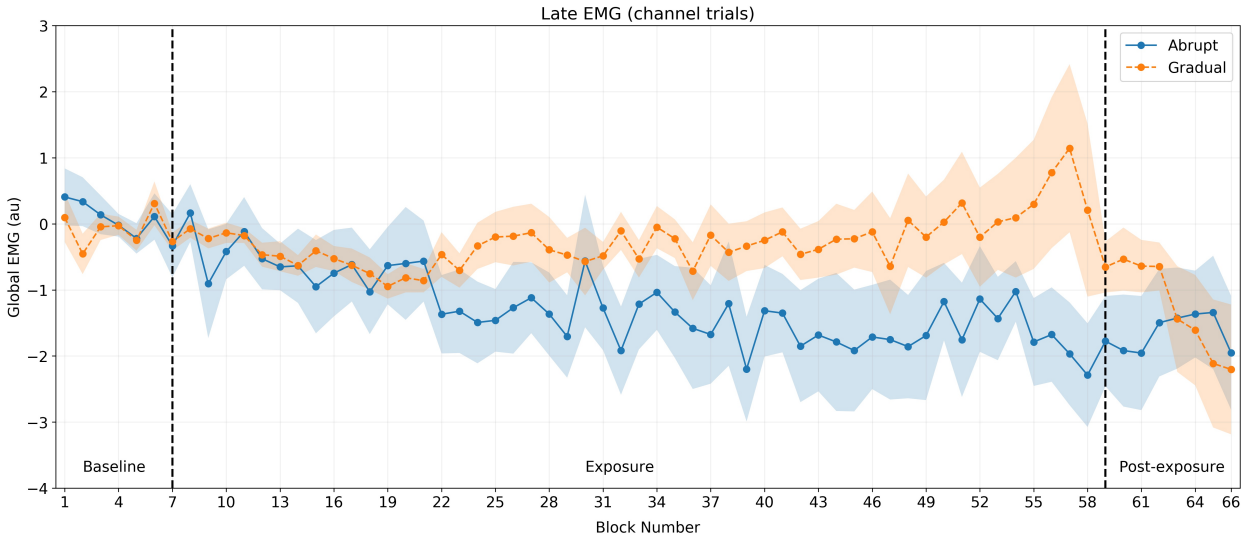

Figure 7: Global EMG of channel trials during the late EMG period. Global EMG is in arbitrary units (au). Data shows mean ± standard error.

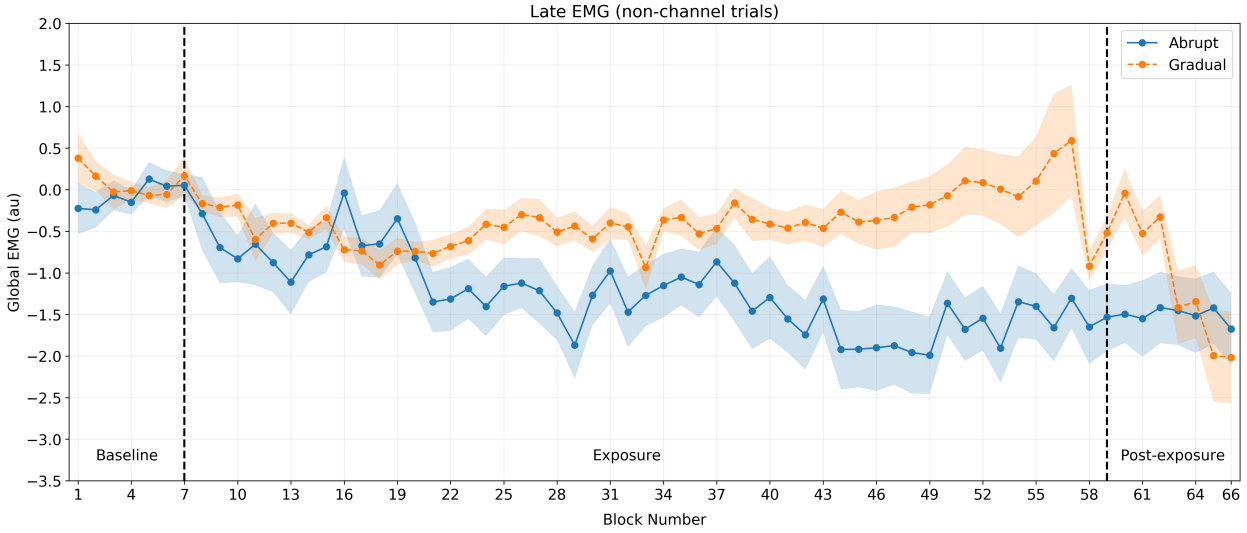

Figure 8: Global EMG of non-channel trials during the late EMG period. Global EMG is in arbitrary units (au). Data shows mean ± standard error.

In order to compare the group and time effect between the two groups from early to late post-exposure, we performed a repeated measures ANOVA. For the early EMG period of the channel trials between the two groups, there was no main effects of time ($F_{1,13} = 1.457$, $P = 0.249$) or group ($F_{1,13} = 0.021$, $P = 0.886$) nor a group by time interaction ($F_{1,13} = 3.118$, $P = 0.101$).

The non-channel trials likewise displayed no main effect of time ($F_{1,13}$ = 1.299, P = 0.275) or group ($F_{1,13}$ = 0.128, P = 0.726) or a group by time interaction ($F_{1,13}$ = 1.195, P = 0.294). Similar results were observed for the late period of the channel trials and non-channel trials. There was no significant effect for time ($F_{1,13}$ = 1.301, P = 0.275), group ($F_{1,13}$ = 0.186, P = 0.673) or group by time interaction ($F_{1,13}$ = 2.620, P = 0.130) for the channel trials. The non-channel trials

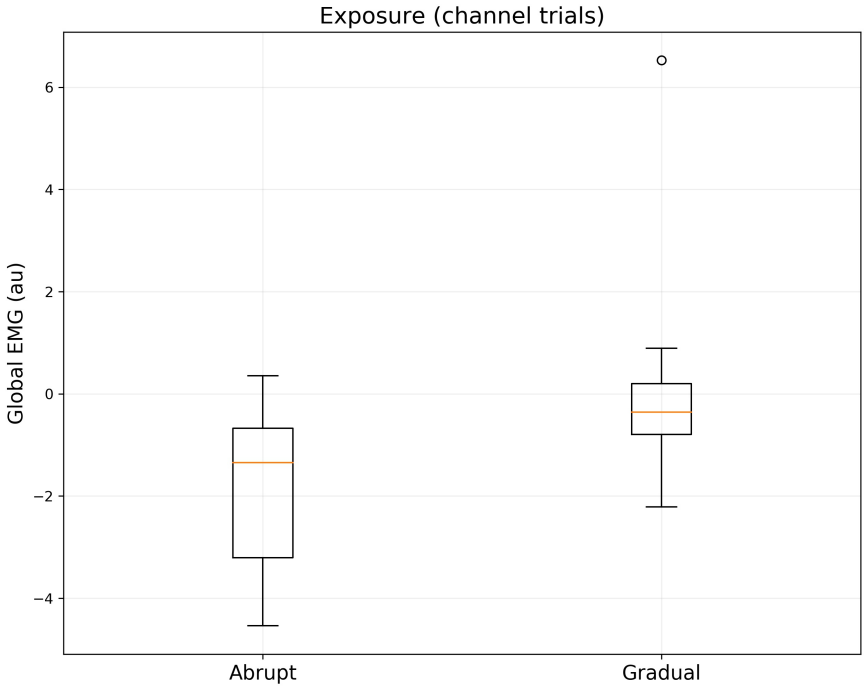

Figure 9: Global EMG of channel trials (late period of EMG) during the exposure phase.

of the late EMG period displayed no main effect for time ($F_{1,13}$ = 1.767, P = 0.207), group ($F_{1,13}$ = 0.360, P = 0.559) and no interaction between group and time ($F_{1,13}$ = 1.546, P = 0.236).

An independent sample t-test of the late period EMG during late post-exposure (last 12 trials – 9 non-channel trials, 3 channel trials) revealed that there was no difference between the groups for the channel (abrupt: n = 7, -1.553 ± 2.013; gradual: n = 8, -1.975 ± 2.371; two-tailed t-test: t_{13} = 0.369, P = 0.718) and non-channel (abrupt: n = 7, -1.537 ± 2.033; gradual: n = 8, -1.786 ± 2.370; two-tailed t-test: t_{13} = 0.216, P = 0.832) trials. As expected, after the force field is removed, the aftereffects are seen for a short time and the level of co-contraction returns to a similar level again.

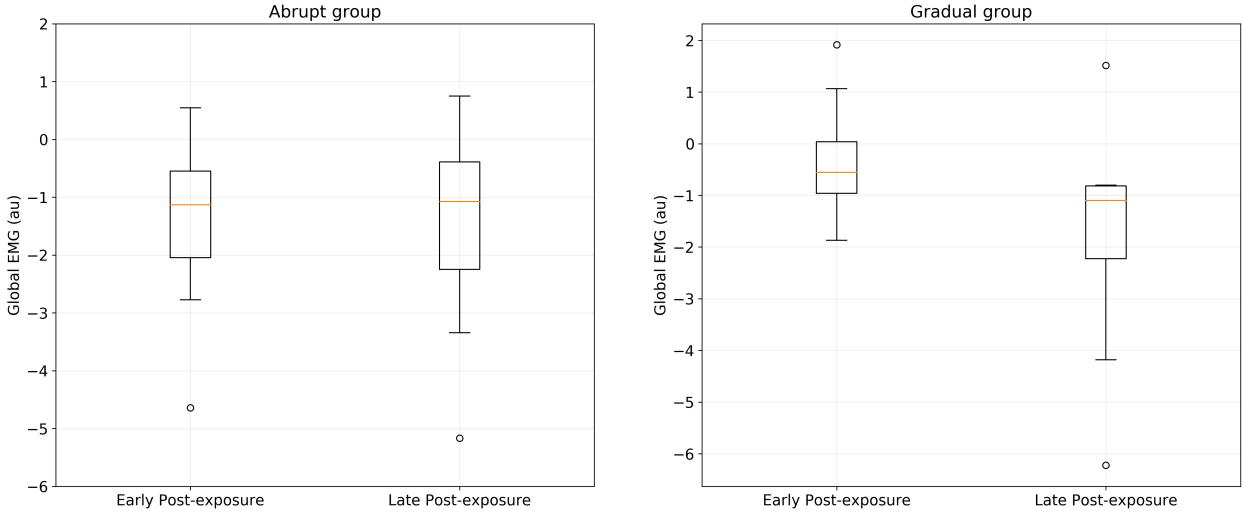

Figure 10: Global EMG of non-channel trials (late period of EMG) during early and late post-exposure phase.

CHAPTER 6

DISCUSSION

Using a center-out reaching paradigm with a velocity-dependent force field, we found that when force perturbations were introduced during exposure, both the abrupt and the gradual group displayed a similar level of muscle co-contraction. As the trials progressed, a tendency to co-contract more was present in the gradual group. In the early part of post-exposure, this tendency of the gradual group to co-contract more than the abrupt group prevailed. Towards the later part of post-exposure, the aftereffects disappear, and co-contraction becomes similar between the two groups.

In the context of the quality of adaptation, studies have shown that gradual dynamic perturbations can be more effective than abrupt perturbations [Kagerer et al., 1997; Klassen et al., 2005]. Concurrently, it has been hypothesized that muscle co-contraction accelerates the rate of internal model acquisition during reaching movements in the presence of novel dynamics [Heald et al., 2018]. Therefore, we hypothesized that if muscle co-contraction fastens internal model acquisition and adaptation to the task, participants in the gradual perturbation group would display a higher level of muscle co-contraction than participants in the abrupt perturbation group. If this was the case, it would support the notion that muscle co-contraction can be an important contributor to internal model acquisition.

Muscle co-contraction can be measured through multiple methods. We examined it using two methods – i) Co-contraction Index and ii) Global EMG. In the course of the data analysis, we decided to focus more on the Global EMG method than on the CI method, for the following reason: Since the isometric MVC EMG signals did not correspond to maximal contraction in some instances, the normalized EMG signals consequently were on a different scale across participants and was therefore not valid for comparisons between the participants. Due to this reason, the global EMG was the primary measure used to draw conclusions in this study.

In the previous study using the same data, EMG signals were segmented into 500 ms

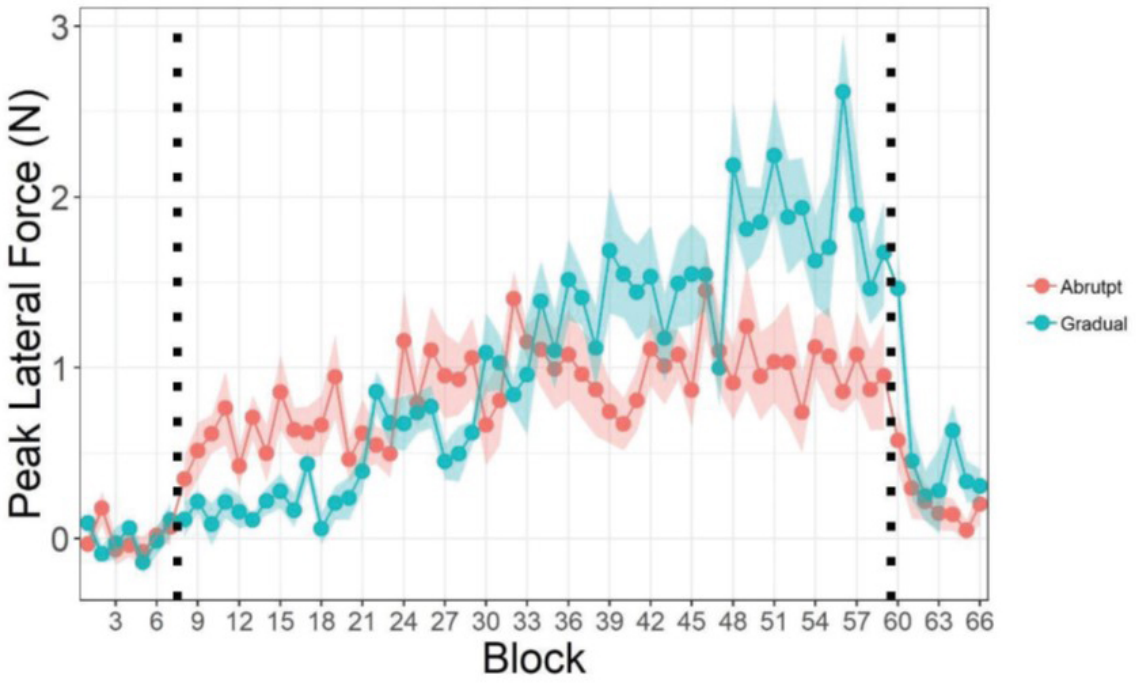

Figure 11: Plot of PLF over the course of the experiment from the previous study [Ptashnik, 2019]. Data shows the mean ± standard error across the two groups.

blocks and an integral of the signal was taken. This method did not follow the filtering frequency, or the methods suggested by the ISEK standards. No quantitative measure of co-contraction was calculated, and this study aimed to address these limitations.

The previously analyzed kinematic data from the study indicated that participants in the gradual perturbation group did in fact show better adaptation than those in the abrupt perturbation group.This was shown, for example, in the kinematic data through peak lateral force (PLF). PLF, as seen in Figure 11, was recorded during the so-called channel trials in every block. Approximately every fourth trial was a channel trial, and only movements to the 90° target were used for such trials. There was no perturbation in these trials, but the movement was constrained by a virtual force channel that allowed participants only to move in a straight trajectory, while the force exerted against the channel walls was recorded; these trials served as probes to measure adaptation to the perturbation. PLF was close to zero for both the groups during baseline. Post-hoc comparisons revealed that PLF was similar between the two groups during early exposure but differed significantly

towards the end of exposure with the gradual group demonstrating a better adaptation. Analysis of the second block of post-exposure revealed that the gradual group maintained a higher PLF than the abrupt group. Based on our hypothesis and results from the previous study, we expected the gradual group to display a higher level of co-contraction than the abrupt group.

We examined global EMG over two periods (early and late), two types of trials (channel and non-channel) and three phases (late exposure, early post-exposure and late post-exposure). Both the abrupt and gradual group displayed a similar level of co-contraction during the baseline phase as seen in Figures 5, 6, 7 and 8. As both the groups made reaches in a null field, we expected them to display identical co-contraction, particularly towards the later part of baseline as they get used to the task. The figures also display co-contraction after the introduction of dynamic perturbations during exposure. While the level of co-contraction was identical between the two groups early in exposure, it can be seen that the level of the abrupt group slowly decreased. On the other hand, there was an increase in co-contraction with the gradual group as the trials progressed and the strength of the force field increased. During late exposure (last 20 trials of exposure), our results indicate a clear tendency of the gradual group to co-contract more than the abrupt group. This tendency could be due to the need to maintain stability and meet precision demands as the gradual group encountered a stronger force field every 52 trials; this finding aligns with the PLF results from the kinematic analysis. PLF between the groups was not different during initial exposure but differed significantly during late exposure. This was an indication of better adaptation by the gradual group as the trials progress. As muscle co-contraction follows the same pattern, it might be indicative that it facilitates better adaptation.

In the early EMG period of exposure, the gradual group exhibited an inclination to co-contract more than the abrupt group. The early EMG period is a measure of feedforward control; as the internal model is refined during the exposure phase, it is getting better at predicting the dynamics. As the strength of the force field increases gradually, the sensorimotor circuitry, through feedback processes, increases muscle co-contraction to counter the predicted dynamics and accelerate internal model acquisition.

For the post-exposure phase, even though results of the repeated measures ANOVA did not indicate any main effects of time, group or any group by time interaction, the individual samples t-test of early post-exposure (initial 12 trials of post-exposure) revealed that the gradual group co-contracted more. However, during late post-exposure (last 12 trials of post-exposure), the results suggested no difference in co-contraction between the two groups. Previous studies have concluded that this aftereffect (or adaptation) exists only for a short period of time, and our results agree with this. During early post-exposure, the gradual group tended to display a higher level of co-contraction than the abrupt group. A higher level of adaptation, as seen in the kinematic data with the PLF, is accompanied by higher co-contraction. As the trials progressed, there was no difference in co-contraction during the late post-exposure phase. Visual inspection of the data in Figures 5, 6, 7 and 8 suggest that the EMG data might support the hypothesized connection between co-contraction and adaptation. Despite of the earlier mentioned shortcomings of the CI method, the pattern of the aftereffects observed in post-exposure was very similar to the one observed in the global EMG method.

In conclusion, using the global EMG approach, the data suggest that muscle co-contraction may be one of the mechanisms used by the CNS for better updating of the internal model resulting in more efficient adaptation. Differences were observed between the results of our study and that by Heald et al. [2018]. These might be due to the discrepancy between the experiment paradigms. The three targets in our study were oriented at 45°, 90° and 135° as opposed to the four targets at 0°, 90°, 180° and 270° for the study by Heald et al. [2018]. The variance in the distance to the target (10 cm in our study as opposed to 12 cm in the other study) and reach times targeted (between 800 ms and 1250 ms in our study versus 200 ms to 300 ms in the Heald et al. [2018] study) might also be a contributing factor in the difference between the two results. The baseline phase of the study by Heald et al. [2018] comprised of 100 null field trials between 36 participants and provided a better baseline value to compute global EMG. Alternatively, a better designed protocol to obtain maximal isometric contraction for MVC EMG could aid the validity of the results from the CI method. Analysis of results from both the CI method and the global EMG method can be

suggestive of the role of muscle co-contraction in internal model acquisition and motor learning.

BIBLIOGRAPHY

BIBLIOGRAPHY

Bowsher, K. A., Damiano, D. L., and Vaughan, C. L. (1993). Joint torques and co-contraction during gait for normal and Cerebral Palsy children. *Journal of Biomechanics*, 26(3):326. Publisher: Elsevier.

Brashers-Krug, T., Shadmehr, R., and Bizzi, E. (1996). Consolidation in human motor memory. *Nature*, 382(6588):252–5. Num Pages: 2 Place: London, United States Publisher: Nature Publishing Group.

Burden, A. and Bartlett, R. (1999). Normalisation of EMG amplitude: an evaluation and comparison of old and new methods. *Medical Engineering & Physics*, 21(4):247–257.

Burden, A. M., Trew, M., and Baltzopoulos, V. (2003). Normalisation of gait EMGs: a re-examination. *Journal of Electromyography and Kinesiology*, 13(6):519–532.

Chow, J. W., Yablon, S. A., and Stokic, D. S. (2012). Coactivation of ankle muscles during stance phase of gait in patients with lower limb hypertonia after acquired brain injury. *Clinical Neurophysiology*, 123(8):1599–1605.

Damiano, D. L., Martellotta, T. L., Sullivan, D. J., Granata, K. P., and Abel, M. F. (2000). Muscle force production and functional performance in spastic cerebral palsy: Relationship of cocontraction. *Archives of Physical Medicine and Rehabilitation*, 81(7):895–900.

Darainy, M. and Ostry, D. J. (2008). Muscle cocontraction following dynamics learning. *Experimental Brain Research*, 190(2):153–163.

De Luca, C. J., Donald Gilmore, L., Kuznetsov, M., and Roy, S. H. (2010). Filtering the surface EMG signal: Movement artifact and baseline noise contamination. *Journal of Biomechanics*, 43(8):1573–1579. Num Pages: 1573-1579 Place: Kidlington, United Kingdom Publisher: Elsevier Limited.

Fitts, P. M. (1992). The information capacity of the human motor system in controlling the amplitude of movement. *Journal of Experimental Psychology: General*, 121(3):262–269. Num Pages: 262-269 Place: Washington, US Publisher: American Psychological Association (US).

Francis, B. A. and Wonham, W. M. (1976). The internal model principle of control theory. *Automatica*, 12(5):457–465. Publisher: Pergamon.

Gribble, P. L., Mullin, L. I., Cothros, N., and Mattar, A. (2003). Role of Cocontraction in Arm Movement Accuracy. *Journal of Neurophysiology*, 89(5):2396–2405. Publisher: American Physiological Society.

Gribble, P. L. and Ostry, D. J. (1998). Independent coactivation of shoulder and elbow muscles. *Experimental Brain Research*, 123(3):355–360.

Harris, C. M. and Wolpert, D. M. (1998). Signal-dependent noise determines motor planning. *Nature*, 394(6695):780–4. Num Pages: 780-4 Place: London, United States Publisher: Nature Publishing Group.

Heald, J. B., Franklin, D. W., and Wolpert, D. M. (2018). Increasing muscle co-contraction speeds up internal model acquisition during dynamic motor learning. *Scientific Reports*, 8.

Hesse, S., Brandl-Hesse, B., Seidel, U., Doll, B., and Gregoric, M. (2000). Lower limb muscle activity in ambulatory children with cerebral palsy before and after the treatment with Botulinum toxin A. *Restorative Neurology & Neuroscience*, 17(1):1. Publisher: IOS Press.

Ito, M. (1984). *The Cerebellum and Neural Control*. Raven Press. Google-Books-ID: Wt1qAAAAMAAJ.

Kagerer, F. A., Contreras-Vidal, J. L., and Stelmach, G. E. (1997). Adaptation to gradual as compared with sudden visuo-motor distortions. *Experimental Brain Research*, 115(3):557–561.

Kawato, M. (1999). Internal models for motor control and trajectory planning. *Current Opinion in Neurobiology*, 9(6):718–727.

Kellis, E., Arabatzi, F., and Papadopoulos, C. (2003). Muscle co-activation around the knee in drop jumping using the co-contraction index. *Journal of Electromyography and Kinesiology*, 13(3):229–238.

Klassen, J., Tong, C., and Flanagan, J. R. (2005). Learning and recall of incremental kinematic and dynamic sensorimotor transformations. *Experimental Brain Research*, 164(2):250–259.

Merletti, R. (2018). Standards for Reporting EMG Data. *Journal of Electromyography and Kinesiology*, 42:I–II.

Miall, R. C. and Wolpert, D. M. (1996). Forward Models for Physiological Motor Control. *Neural Networks*, 9(8):1265–1279.

Milner, T. E. (2002). Adaptation to destabilizing dynamics by means of muscle cocontraction. *Experimental Brain Research*, 143(4):406–16. Num Pages: 11 Place: Heidelberg, Netherlands Publisher: Springer Nature B.V.

Milner, T. E. and Franklin, D. W. (2005). Impedance control and internal model use during the initial stage of adaptation to novel dynamics in humans. *The Journal of Physiology*, 567(Pt 2):651–664.

Osu, R., Franklin, D. W., Kato, H., Gomi, H., Domen, K., Yoshioka, T., and Kawato, M. (2002). Short- and Long-Term Changes in Joint Co-Contraction Associated With Motor Learning as Revealed From Surface EMG. *Journal of Neurophysiology*, 88(2):991–1004. Publisher: American Physiological Society.

Powers, S. K. (2020). *Exercise Physiology: Theory and Application to Fitness and Performance*. McGraw-Hill US Higher Ed USE, Columbus, UNITED STATES.

Ptashnik, D. W. (2019). CO-CONTRACTILE DIFFERENCES DURING ADAPTATION TO ABRUPT AND GRADUAL DYNAMIC PERTURBATIONS. page 88.

Rosa, M. (2014). Co-contraction Role on Human Motor Control. A Neural Basis. *Journal of Novel Physiotherapies*, 05(01).

Rosa, M. C. N., Marques, A., Demain, S., Metcalf, C. D., and Rodrigues, J. (2014). Methodologies to assess muscle co-contraction during gait in people with neurological impairment – A systematic literature review. *Journal of Electromyography and Kinesiology*, 24(2):179–191.

Shadmehr, R. and Mussa-Ivaldi, F. (1994). Adaptive representation of dynamics during learning of a motor task. *The Journal of Neuroscience*, 14(5):3208–3224.

Shadmehr, R., Wise, S. P., Wise, N. I. o. M. H. i. B. M. S. P., and Wise, S. P. (2005). *The Computational Neurobiology of Reaching and Pointing: A Foundation for Motor Learning*. MIT Press. Google-Books-ID: fKeImql1s_sC.

Thoroughman, K. A. and Shadmehr, R. (1999). Electromyographic Correlates of Learning an Internal Model of Reaching Movements. *Journal of Neuroscience*, 19(19):8573–8588. Publisher: Society for Neuroscience Section: ARTICLE.

Unnithan, V. B., Dowling, J. J., Frost, G., Volpe Ayub, B., and Bar-Or, O. (1996). Cocontraction and phasic activity during GAIT in children with cerebral palsy. *Electromyography and Clinical Neurophysiology*, 36(8):487–494.

Winter, D. A. (2009). *Biomechanics and Motor Control of Human Movement*. John Wiley & Sons, Ltd, 1 edition. _eprint: https://onlinelibrary.wiley.com/doi/pdf/10.1002/9780470549148.

Wolpert, D. M., Ghahramani, Z., and Jordan, M. I. (1995). An internal model for sensorimotor integration. *Science*, 269(5232):1880+. 1880.

Wolpert, D. M., Miall, R. C., and Kawato, M. (1998). Internal models in the cerebellum. *Trends in Cognitive Sciences*, 2(9):338–347.